J. At. Mol. Sci.
doi: 10.4208/jams.072813.091013a

Vol. **5**, No. 2, pp. 110-122
May 2014

First-principles calculations of the electronic structures and optical properties of Mg- and Sr-doped CaF_2

Fang Peng[a,*], Yu-Feng Peng[a], Guang Zheng[b], and Cong-Cong Zhai[a]

[a] *College of Physics and electronic Engineering, Henan Normal University, Xinxiang 453007, China*
[b] *College of Physics and Information Engineering, Jianghan University, Wuhan 430056, China*

Received 28 July 2013; Accepted (in revised version) 10 September 2013
Published Online 28 February 2014

Abstract. Based on the density functional theory (DFT), the first-principles methods are used to study and compare the electronic structures and optical properties of Mg-, Sr-doped CaF_2 systems with those of CaF_2 bulk in detail. In contrast to CaF_2 bulk, the band gaps of doped systems become narrower and the new peaks of density states appear. The orbital interactions between Mg, Sr atoms and Ca atom are enhanced near the Fermi level, besides, the doped systems all show single dielectric properties and their absorption coefficients for ultraviolet light are reduced greatly, for Ca_7SrF_{16} system, there is a small absorption peak at 25.44 eV. Compared with CaF_2 bulk, doped systems have much lower extinction coefficients and much higher light transmittance in the ultraviolet region. In addition, their reflection and loss peaks all display red shift and the peak value reduce.

PACS: 31.15.E-, 71.20.-b, 78.20.-e

Key words: density functional theory, electronic structure, optical property, dope

1 Introduction

Calcium fluoride (CaF_2) crystals have been widely used as optical medium materials for many years due to their excellent properties such as high transmittance and broad transmittance range (from far UV to mid-IR), low refractive index, high chemical resistance and high laser damage threshold [1]. Recently, large size CaF_2 crystals are required as an important lens material for photolithographic processing of silicon integrated circuits (IC) at wavelengths in the deep ultraviolet (DUV) region [2]. Calcium fluoride crystals

*Corresponding author. *Email address:* zpfzyyx@163.com (F. Peng)

have so many advantages that attract a number of scholars to research into them [3-8]. Calcium fluoride has typical fluorite structure consisting of a simple cubic array of fluorine ion (F-) with every alternate cube occupied by calcium ion (Ca^{2+}). This kind of fluorite structure enables high doping concentration of foreign ions, especially for doped with transition-metal and rare-earth ions. For CaF_2 doped systems, the changes in electronic structures and optical properties can introduce new characters different from those of CaF_2 bulk. For example, in the case of CaF_2:Yb single crystal thanks to its broad emission bands, it shows very good performances as tuneable laser and as ultra-short pulse laser generator [9,10]. Recently, the synthesis and upconversion luminescence properties of Er^{3+}:CaF_2 nanoparticles co-doped with Yb^{3+} as sensitizer were reported [11]. Lately, high power diode-pumped femtosecond laser as well as self-Q-switched laser based on Yb doped and Na-Yb co-doped CaF_2 crystals were developed [12]. Light emitting structures based on nanocrystalline Si/CaF_2 system were developed featuring a great dependence of the photoluminescence properties from the nanoparticles size [13]. Additionally, there are other literatures about synthesis of CaF_2 nanoparticles or hollow sphere doped with rare-earth and alkaline-earth ions, such as Eu^{3+} [14,15], Tb^{3+} [16,17] and Ce^{3+} [18] were successively reported. Besides, Magnesium(Mg) and Strontium(Sr) doped calcium fluoride nanocrystals were synthesized by co-precipitation method by C. Pandurangappa [19], for Mg:CaF_2 and Sr:CaF_2 nanocrystals, their morphological features, optical absorption spectrum and photoluminescence spectrum were studied in detail. However, in the experiment, there would be interaction among elements in the interface between metals and calcium fluoride films, which may affect the structures and optical properties of CaF_2 doping systems, so there are limitations in the experimental research and the computational simulation at the atomic level is particularly important. Currently, theoretical reports on the physical mechanism about the crystal structures, electrical and optical properties of Mg-, Sr-doped CaF_2 systems are very rare.

In this paper, using the first-principles methods based on the density functional theory (DFT), we have studied the electronic structures and optical properties of CaF_2 bulk and Mg-, Sr-doped CaF_2 systems. To be specific, we have calculated the total density of states (DOS) and partial density of states (PDOS), the real and imaginary parts of complex dielectric functions, absorption coefficients, refractive indexes, extinction coefficients, reflectivity and loss functions. The present results are compared with the available experimental results. Our results would play a guiding role in preparation and development in the field of application about Mg-, Sr-doped CaF_2 systems.

2 Theoretical systems and calculation method

2.1 Theoretical systems

CaF_2 bulk belongs to cubic fluorite structure, its space group is Fm 3m and lattice constants $a(b,c)$ are 5.4630 Å [20]. The unit cell of CaF_2 is composed by four calcium atoms and eight fluorine atoms, there is equal bond length between each calcium atom and each

fluorine atom in the nearest close-packed planes. In this paper, we select 2x1x1 CaF_2 supercell consisting of 24 atoms as the calculated system with formula Ca_8F_{16}, of which a Ca atom is replaced by Cr, Mo and W atoms respectively with doping concentration 12.5%. The molecular formulas are Ca_7MgF_{16} and Ca_7SrF_{16}, their structure models are shown in Fig. 1.

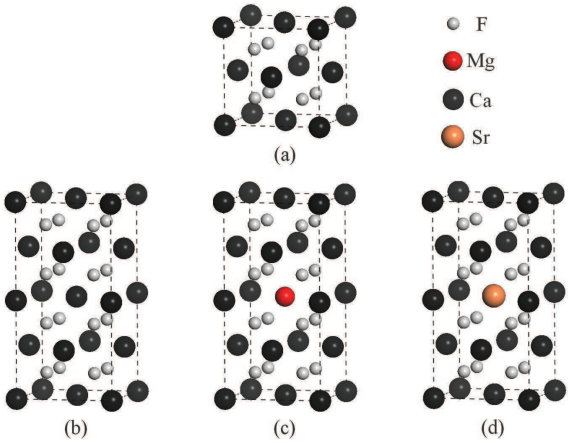

Figure 1: Crystal structures of CaF_2 bulk and doped systems. (a) CaF_2 bulk, (b) Ca_8F_{16} system, (c) Ca_7MgF_{16} system, (d) Ca_7SrF_{16} system.

2.2 Calculation method

Our simulations are performed with the Cambridge serial total energy package (CASTEP) code, which is based on DFT using a plane-wave pseudopotential method [21]. The generalized gradient approximation (GGA) in the scheme of Perdew-Burke-Ernzerhof (PBE) is used to treat the exchange-correlation function [22]. In order to make the wave function become more smooth, then reduce the cutoff energy and calculated amount, we use the ultrasoft pseudopotential [23] to describe the electro-ion interaction. The valence-electron configurations for the Ca, F, Mg and Sr atoms respectively are Ca $4s^2$, F $2s^22p5$, Mg 3s2 and Sr 5s2. The plane-wave functions of valence electrons are expanded in a plane-wave basis set. Reciprocal-space integration over the first Brillouin zone is approximated through a careful sampling at a finite number of k points using a Monkhorst-Pack mesh [24]. In our calculation, the cut-off energy has been assumed to be 500 eV. Self-consistency is considered to be achieved when the charge density difference between succeeding interactions is less than 2×10^{-6} eV/atom, and the geometries are considered to be converged when the forces on each ions becomes 0.03 eV/Å (1 Å=0.1 nm) or less. In the optimization process, the maximum stress is set to 0.05 GPa. Our calculated structural parameters of CaF_2 bulk are listed in Table 1. The results are in good agreement with the available experimental results [20] and the theoretical reference [25], which show that our calculation method is reliable. Besides, the optimized structural parameters of 2x1x1

CaF_2 supercell and doped systems are shown in Table 2, Compared with CaF_2 supercell, the volume of Ca_7MgF_{16} becomes smaller, the bond length between each Mg atom and F atom in the nearest close-packed planes is shorter, this is due to that the radius of Mg^{2+} is less than that of Ca^{2+}. But for Ca_7SrF_{16} system, the radius of Sr^{2+} is larger than that of Ca^{2+}, so its volume is larger than that of CaF_2 bulk, and the bond length between each Sr atom and F atom in the nearest close-packed planes is longer. To sum up, there are obvious structural changes after CaF_2 bulk doped with Cr, Mo and W atoms.

Table 1: Lattice constants $a(b,c)$, bond length d_{Ca-F} between each calcium atom and fluorine atom in the nearest close-packed planes, and bulk modulus B for CaF_2 bulk.

	$a(b,c)$ / Å	d_{Ca-F} / Å	B(GPa)
This work	5.5106	2.386	84
Experiment[20]	5.4630	2.365	82.71
Reference[25]	5.5637	-	-

Table 2: Lattice constants, bond length between each X (Ca, Mg, Sr) atom and F atom in the nearest close-packed planes, and band gaps for optimized 2x1x1CaF_2 supercell and doped systems.

Systems	a / Å	$b(c)$ / Å	c/a	d_{X-F} / Å	Eg / eV
2x1x1CaF_2	11.023	5.5117	0.5000	2.3866	7.124
Ca_7MgF_{16}	10.922	5.4565	0.4996	2.2721	6.702
Ca_7SrF_{16}	11.120	5.5562	0.4997	2.4771	6.997

3 Results and discussion

3.1 Band structures and density of states

Based on the optimized structures, the band structures, DOS and PDOS of CaF_2 bulk and doped systems are shown in Fig. 2 and Fig. 3 respectively. For CaF_2 bulk, the highest energy of valence bands and the lowest energy of conduction bands are both located at Γ(G) point, its direct gap is seen to be 7.124 eV, which is in accordance with the theoretical result 7.07 eV reported by Verstraete M and Gonze X [25]. Experimentally, the direct band gap is 12.1 eV and the indirect gap is estimated to be 11.8 eV [26]. Compared with the experimental value, our calculated band gap is lower. As we know, DFT belong to the ground-state theory and systematically underestimate the band gap in many-body system, which affect the level distribution of electronic state and the energy of interband transition among electrons, but they don't affect the qualitative analysis and comparison about the electronic structure and optical properties. For Ca_7MgF_{16} and Ca_7SrF_{16} systems, whose highest energies of valence bands and lowest energies of conduction bands are located at different points, their indirect gaps are 6.702 eV and 6.997 eV respectively. Compared with CaF_2 bulk, the band gaps of doped systems narrow, the reason is that orbital interactions between Mg 2p3s, Sr 3d atates and Ca 3d state are enhanced, which leads to the conduction bands moving to the low level.

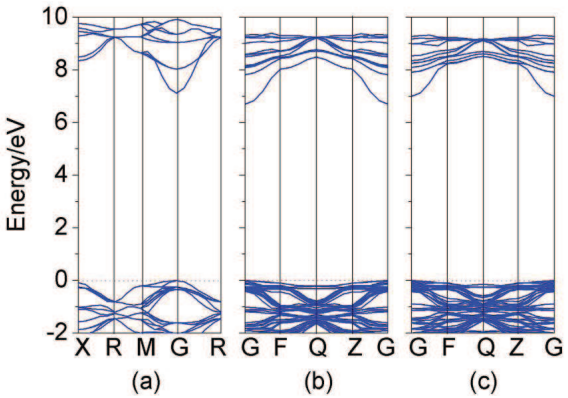

Figure 2: Band structures of CaF_2 bulk and doped systems. (a) CaF_2 bulk, (b) Ca_7MgF_{16} system, (c) Ca_7SrF_{16} system

To gain more insight on the difference between the crystal structures and the bonding characteristics about Mg- and Sr-doped CaF_2 systems, we investigate the DOS and PDOS of CaF_2 bulk and doped systems as shown in Fig. 3. From Fig. 3(a) we know that there are five intervals for DOS of CaF_2 bulk, in the conduction band (CB), the region located between 6.9 eV and 10.8 eV is mostly dominated by Ca 3d state, the lowest valence band (VB) around -36.9 eV to -35.1 eV is constituted by Ca 4s state, the next band ranging from -20.8 eV to -15.6 eV is divided into two narrow sub-bands and they are mainly composed of F 2s and Ca 3p states. Finally, the band in the range of -3.1D 0.8 eV near the Fermi level is mainly formed with F 2p state. Fig. 3(b, c) display the DOS and PDOS of Mg- and Sr-doped CaF_2 systems, for doped systems, the peak positions of DOS owing to the contributions of 2s, 2p states of F atom and 4s, 3p states of Ca atom in the valence bands are roughly the same as those of CaF_2 bulk. In contrast to CaF_2 bulk, for Ca_7MgF_{16} system, there is new peak of DOS formed with Mg 2p state around -39.8 eV–38.1 eV. The two new peaks of DOS of Ca_7SrF_{16} system in the valence band are located at 30.7D -29.0 eV and 12.7D -11.0 eV, which are mainly constituted by 5s and 4p states of Sr atom respectively. The new peaks of DOS of doped systems correspond to the low level and they are relatively separate, so the interaction with other valence band is weak and the influence on the system is few. Besides, for doped systems, whose peaks of DOS around 8 eV in the conduction bands are primarily formed with 3d state of Ca atom, as well as small contributions of 2p3s states of Mg atom and 3d state of Sr atom, and there are orbital interactions between Ca 3d and Mg 2p3s orbits and Sr 3d orbit.

Fig. 3(d) shows the DOS of CaF_2 bulk and doped systems near the Fermi level. We learn that the peaks of DOS of three configurations near the Fermi level are mostly dominated by 2p state of F atom. For Ca_7MgF_{16} and Ca_7SrF_{16}, there are also small contributions of 2p3s states of Mg atom and 3d state of Sr atom. Compared with CaF_2 bulk, there are phenomena that the orbital interactions between Ca atom and doped atoms are enhanced weakly, which indicate that the Mg and Sr atoms slightly change the bonding

characteristics of crystals. Moreover, the band widths of doped systems are roughly the same as that of CaF_2 bulk, which shows that the nonlocality of electrons and the expansibility of atomic orbitals near the Fermi level are unchanged.

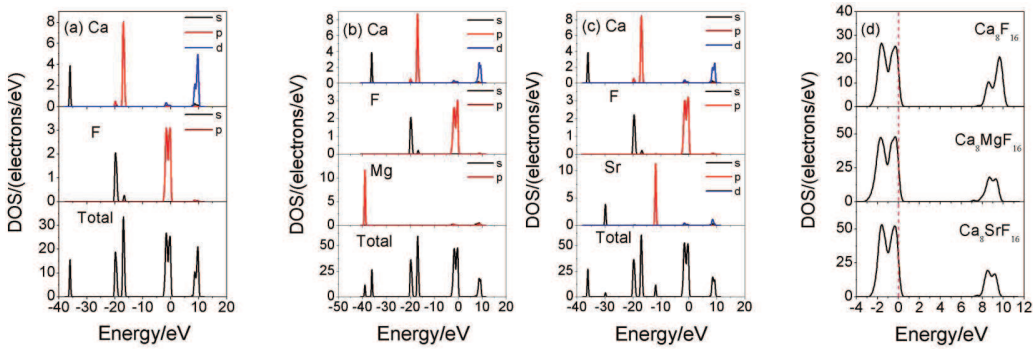

Figure 3: Total DOS and PDOS of CaF_2 bulk and doped systems. (a) CaF_2 bulk, (b) Ca_7MgF_{16} system, (c) Ca_7SrF_{16} system, (d) the DOS near Fermi level.

3.2 Optical properties

The macro-optical response functions of solid usually are described by complex refractive index in linear response range, which is described by the following equation

$$N(\omega)=n(\omega)+ik(\omega) \tag{1}$$

According to the definition of direct transition probability and the kramers-Kronig relation, we can deduce the crystal refractive index $N(\omega)$, absorption coefficient $\alpha(\omega)$ and so on [27]. The formulas are as follows

$$\varepsilon_2=\frac{4\pi^2}{m^2\omega^2}\sum_{V,C}\int_{BZ}d^3k\frac{2}{2\pi}|eM_{CV}(K)|^2\times\delta[E_C(K)-E_V(K)-\hbar\omega] \tag{2}$$

$$\varepsilon_1=1+\frac{8\pi^2e^2}{m^2}\sum_{V,C}\int_{BZ}d^3k\frac{2}{2\pi}\frac{|eM_{CV}(K)^2|}{[E_C(K)-E_V(K)]}\times\frac{h^3}{[E_C(K)-E_V(K)]^2-\hbar^2\omega^2} \tag{3}$$

$$n(\omega)=\frac{1}{\sqrt{2}}[(\varepsilon_1^2+\varepsilon_2^2)^{1/2}+\varepsilon_1]^{1/2} \tag{4}$$

$$K(\omega)=\frac{1}{\sqrt{2}}[(\varepsilon_1^2+\varepsilon_2^2)^{1/2}-\varepsilon_1]^{1/2} \tag{5}$$

$$\alpha(\omega)=\frac{4\pi K(\omega)}{\lambda_0} \tag{6}$$

Here ε_1 is the real part and ε_2 is the imaginary part of dielectric function. C and V represent the conduction band and valence band. ł is the reciprocal lattice vector, $E_C(K)$

and $E_V(K)$ are corresponding to the intrinsic levels of the conduction band and valence band. BZ is the first Brillouin zone and $|eM_{CV}(K)|^2$ is the matrix element of momentum transition. In addition, ω is the angular frequency and λ_0 is the wavelength of light in vacuum. These fundamental relations reflect the light-emitting mechanism that spectra are produced by electronic transitions among energy levels, which are the theoretical basis to analyze the optical properties of crystals.

From above formulas we know that other optical parameters could be deduced from $\varepsilon_1(\omega)$ and $\varepsilon_2(\omega)$. As we know, the complex dielectric function $\varepsilon(\omega)$ plays a pivotal role in characterization about the physical properties of materials and is treated as a bridge to connect the microscopic models of physical processes with micro electronic structures of solid. Firstly we analyze the dielectric functions of CaF_2 bulk and doped systems, and then we study their absorption coefficients, refractive indexes, extinction coefficients, reflectivity and loss functions respectively. The optical properties are deduced from the matrix element of momentum transition of electron transition between occupied states and unoccupied states, so whether the band structures are accurate or not which has a great influence on the calculated results, optical properties calculated in the paper are scissors corrected [28,29] by value 4.976 eV, which is the difference in band gap between our value (7.124 eV) and experimental result (12.1 eV). For Mg- and Sr-doped CaF_2 systems, there are no experimental reference values about their band gaps, so doped systems are not scissors corrected. Table 3 displays a series of experimental optical parameters, from Table 3 we acquire that our calculated optical properties of CaF_2 bulk are approximately in accordance with the experimental results [30-33]. For Mg- and Sr- doped CaF_2 systems, C. Pandurangappa et al [19] studied their morphological features, optical absorption spectrum and photoluminescence spectrum. In addition, there is no few report on the optical properties of Mg- and Sr- doped CaF_2 systems, so we analyze a series of optical properties of doped systems through making comparison with those of CaF_2 bulk.

Table 3: Experimental and calculated values of $\varepsilon_1(0)$, $n(0)$, optical absorption edge $\alpha_{edge}(\omega)$, the positions of the first absorption peak $P_{\alpha(\omega)}$ and the first reflection peak $P_{R(\omega)}$ about CaF_2 bulk.

CaF_2	This work	Experiment
$\varepsilon_1(0)$	1.39	-
$n(0)$	1.18	1.26[30]
$\alpha_{edge}(\omega)$	10.55 eV	12.00 eV [31]
$P_{\alpha(\omega)}$	15.55 eV	11.12 eV[32]
$P_{R(\omega)}$	17.00 eV	11.02 eV [33]

3.2.1 Complex dielectric functions of CaF_2 crystal and doped systems

Fig. 4 displays the real parts $\varepsilon_1(\omega)$ and the imaginary parts $\varepsilon_2(\omega)$ of dielectric functions of CaF_2 bulk and doped systems, of which the illustrations show the experimental real

part $\varepsilon_1(\omega)$ and imaginary part $\varepsilon_2(\omega)$ of dielectric function of cleaved $CaF_2(111)$ at room temperature [32]. We can know that our calculated $\varepsilon(\omega)$ curve trends of CaF_2 bulk are roughly in accordance with the experimental curve trends. $\varepsilon_1(\omega)$ is the static dielectric constant of materials when ω is zero, we get the $\varepsilon_1(0)$ of CaF_2 bulk is 1.39, for Ca_7MgF_{16} and Ca_7SrF_{16} configurations, whose $\varepsilon_1(0)$ respectively are 1.21 and 1.19, which are less than that of CaF_2 bulk. As we know, $\varepsilon(\omega)$ curve represents the dielectric properties of materials, we select the point from positive to negative value as the critical value, as shown in the red dotted line I. the materials show the dielectric properties when the photon energy is less than the critical value and display metallicity when the photon energy is greater than that value. We acquire that the $\varepsilon_1(\omega)$ curve trends of doped systems are basically consistent with that of CaF_2 bulk. CaF_2 bulk shows the dielectric properties as well as metallicity. However, the doped systems all show single dielectric properties, so it could keep the dielectric properties after CaF_2 crystal doped with Mg and Sr atoms respectively.

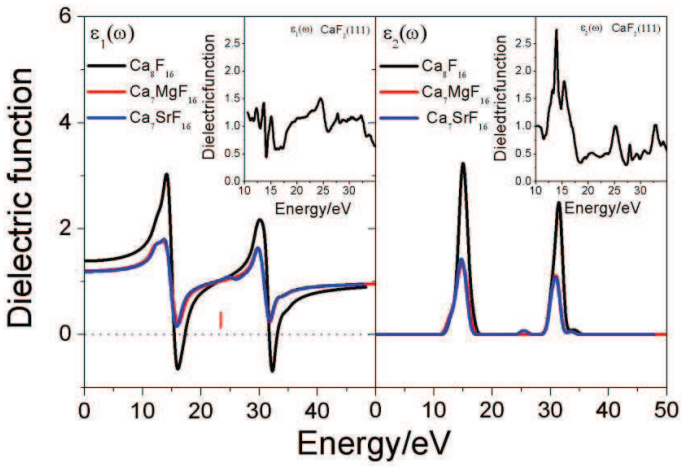

Figure 4: Experimental and calculated real parts $\varepsilon_1(\omega)$, imaginary parts $\varepsilon_2(\omega)$ of dielectric functions of CaF_2 bulk and doped systems.

The threshold energy of $\varepsilon_2(\omega)$ for CaF_2 bulk are 11.18 eV, it is dominated by the direct optical transition from the highest valence band to the lowest conduction band, when the photon energy is greater than this value, the number of possible transition increases sharply and the value of $\varepsilon_1(\omega)$ also increases rapidly. For Ca_7MgF_{16} and Ca_7SrF_{16} systems, their threshold energies produced by indirect optical transition respectively correspond to 10.80 eV and 11.06 eV, they are less than the value (11.18 eV) of CaF_2 bulk. For CaF_2 bulk, its two main peaks of $\varepsilon_2(\omega)$ respectively at 14.08 eV and 30.10 eV. The peak at 14.08 eV should be mainly caused by optical transitions between F 2p state in the highest valence band and Ca 3d state in the lowest conduction band. The peak at about 30.10 eV is formed with the optical transition between F 2p and Ca 4s states. From Fig. 4 we also know that there are both two main peaks of $\varepsilon_2(\omega)$ for doped systems and they are located

at around 14.7 eV and 30.8 eV respectively, the optical-transition modes of two peaks are the same as those CaF_2 bulk. Besides, for Ca_7SrF_{16} system, there is a new peak of $\varepsilon_2(\omega)$ at 25.42 eV, which maybe results from the optical transition between Sr 3dD3d states. Compared with CaF_2 bulk, we find that the main peaks of $\varepsilon_2(\omega)$ show red shift and the peak values decrease. The reason for this phenomenon is that the orbital interaction between Mg 2p3s, Sr 3d states and Ca 3d state are enhanced leading to the conduction band moving to the low level.

3.2.2 Absorption, Refractive indexes, Reflectivity and Loss functions of CaF_2 bulk and doped systems

Calculated absorption coefficients $\alpha(\omega)$, refractive indexes $n(\omega)$, reflectivity spectrums $R(\omega)$ and loss functions $L(\omega)$ of CaF_2 bulk and doped configurations are presented in Fig. 5-8 respectively.

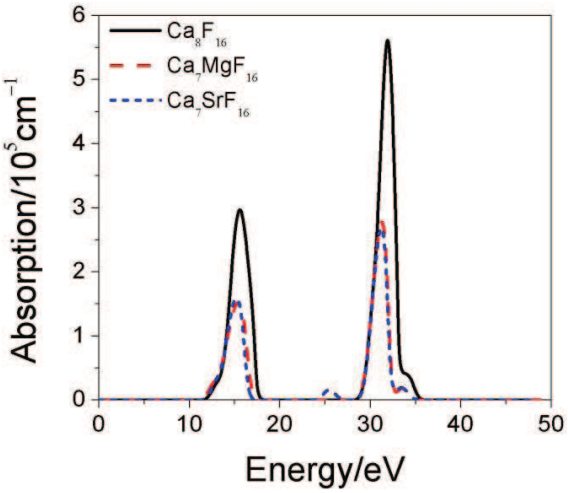

Figure 5: Absorption of CaF_2 crystal and doped systems.

From Fig. 5 we know that the optical absorption edge of CaF_2 bulk lies in the vacuum ultraviolet at 10.55 eV, which is slightly less than the experimental value (12 eV) [31], and the optical absorption edges of Ca_7MgF_{16} and Ca_7SrF_{16} systems respectively are 10.12 eV and 10.39 eV, from these data we acquire that the absorption edges of doped systems slightly move to the direction of the long wave in the ultraviolet region. Besides, we acquire that there are two main peaks of absorption spectra for CaF_2 bulk at 15.55 eV and 31.89 eV, the experimental value about the first absorption band corresponds to 11.12 eV [32], the reason for the difference between our result and experimental value is that the absorption coefficient of CaF_2 bulk is influenced by temperature but theoretical calculation is in the ideal conditions no taking temperature into account. In addition, the absorption coefficient of CaF_2 crystal in the ultraviolet region is very low, which is consistent with the experimental reference [32]. For Ca_7MgF_{16} system, whose two main

absorption peaks respectively locate at 15.40 eV and 31.25 eV, and those of Ca_7SrF_{16} correspond to 15.18 eV and 31.21 eV, moreover, there is a new absorption peak at 25.44 eV for Ca_7SrF_{16} , based on the fact that DFT systematically underestimate the band gap, we think the new absorption peak maybe caused by the optical transition between Sr dDd states, which is consistent with the analysis results of the dielectric function. Combined with the analysis of the band structures, we know that the doped systems not only reduce the band gap but also make the absorption peak expand slightly to the low level, the absorption edge display red shift. Moreover, the absorption coefficients of doped systems are much lower than that of CaF_2 bulk, that is to say, it could greatly reduce the absorption for ultraviolet light after CaF_2 bulk doped with Mg and Sr atoms.

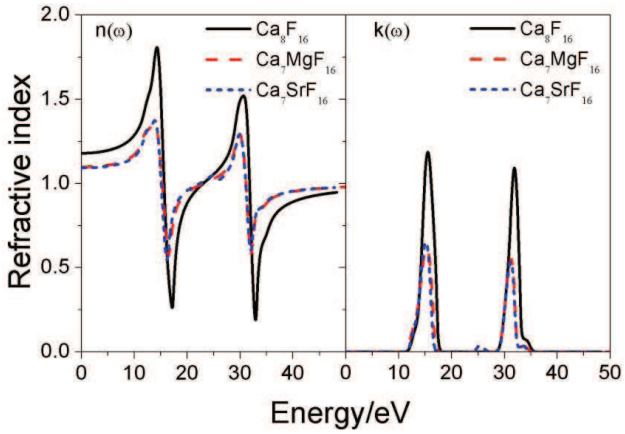

Figure 6: Refractive indexes of CaF_2 crystal and doped systems.

The refractive indexes of CaF_2 bulk and doped systems including $n(\omega)$ and $k(\omega)$ as shown in Fig. 6. The static refractive index n(0) can be got by the limit value of $n(\omega)$. For CaF_2, Ca_7MgF_{16} and Ca_7SrF_{16} configurations, whose n(0) respectively are 1.18, 1.10 and 1.09. The main peaks of $n(\omega)$ of CaF_2 correspond to 14.24 eV and 30.63 eV respectively. In contrast to CaF_2 bulk, $n(\omega)$ peaks of doped systems show red shift and locate at around 13.7 eV and 29.8 eV, besides, the peak values reduce significantly. From Fig. 6 we also acquire that the peaks of extinction coefficient $k(\omega)$ of CaF_2 bulk are mainly located in the ultraviolet region around 11-36 eV, the extinction coefficient of CaF_2 bulk is very low in the visible and ultraviolet regions, which indicates that the light transmittance is high, this is consistent with the experiment reports on the optical properties of CaF_2 crystal [1,32]. Compared with CaF_2 bulk, the peak positions of $k(\omega)$ of doped systems display red shift, moreover, the extinction coefficients of doped systems are much lower and the light transmittances are much higher in the visible and ultraviolet regions, so it could improve the light transmittance especially for ultraviolet light after CaF_2 bulk doped with Mg and Sr atoms.

Fig. 7 and Fig. 8 respectively display the graphs of reflectivity and loss functions of CaF_2 bulk and doped systems, From the figures we know that there are two main re-

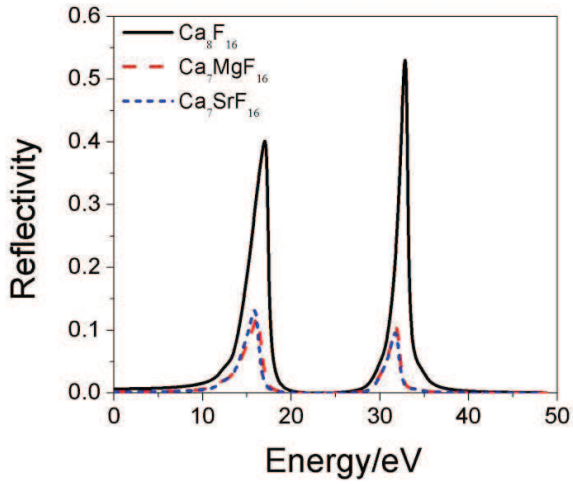

Figure 7: Reflectivity of CaF_2 crystal and doped systems.

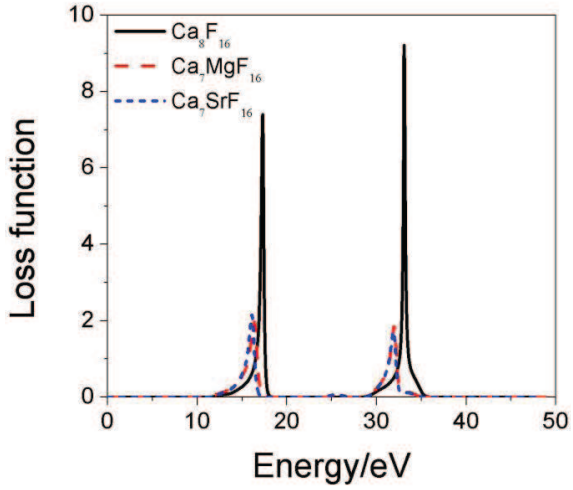

Figure 8: Loss functions of CaF_2 crystal and doped systems.

flection peaks for CaF_2 bulk, which are 0.40 and 0.53 respectively at 17.00 eV and 32.83 eV, the peak at 17.00 eV arises from optical excitation of electrons in the valance and the peak at 32.83 eV is caused primarily by excitations of the core states of Ca^{2+}. The experimental measurements show that the reflection spectra peaks are located in the regions of 6-26 eV and 30-36 eV [32], so our results accord with the experimental values. Compared with CaF_2 bulk, the trends of reflection curves of doped systems are similar, besides, the reflection peaks of doped systems show slight red shift and the peak values decrease significantly, it shows that the optical excitation of electrons and excitations of the core states weaken obviously. Fig. 8 exhibits the loss function $L(\omega)$ which is the physical quantity describing energy loss of electrons in uniform dielectric. The peaks of $L(\omega)$ spectra rep-

resent the characteristic associated with the plasma resonance and the corresponding frequency is the so-called plasma frequency [34]. From Fig. 8 we also acquire that the main peaks of $L(\omega)$ curve of CaF_2 bulk are narrow and sharp, which respectively locate at 17.29 eV and 33.07 eV determining two screened plasma frequencies, at the same time, they correspond to the zero crossing of $\varepsilon_1(\omega)$ and the abrupt reductions of two peaks of reflection spectra. Similarly, for each doped system, there are two main loss peaks also showing plasma frequencies and zero crossing of $\varepsilon_1(\omega)$ with the abrupt reductions of three peaks of $R(\omega)$. Compared with CaF_2 bulk, the loss peaks of doped systems all display red shift and the peak values reduce greatly. To sum up, it could greatly reduce the reflectivity and the energy loss in the ultraviolet region after CaF_2 bulk doped with Mg and Sr atoms.

4 Conclusions

Based on DFT, we use a plane-wave pseudopotential method to study and compare the band structures, electronic and optical properties of doped systems and CaF_2 bulk. The results are as follows

(1) The orbital interactions between Mg 2p3s, Sr 3d states and Ca 3d state are enhanced leading to the band gaps of doped systems narrowing;

(2) There are new peaks of DOS resulting from the orbital transitions of Mg 2p and Sr 5s4p states;

(3) Doped systems show single dielectric properties, their absorption edges display red shift and the peak values reduce significantly;

(4) It could greatly reduce the absorption for ultraviolet light after CaF_2 bulk doped with Mg and Sr atoms;

(5) Doped systems could improve the light transmittance especially for ultraviolet light;

(6) It could greatly reduce the reflectivity and the energy loss in the ultraviolet region after CaF_2 bulk doped with Mg and Sr atoms.

To sum up, our results will be treated as the theoretical guidance for the subsequent experimental research on new performances of CaF_2 doped systems.

Acknowledgments. This work was supported by the National Natural Science Foundation of China (Grant No.61077037).

References

[1] Y. H. Li and G. J. Jiang, J. Synth. Cryst. 29 (2000) 221 (in Chinese).
[2] L. Dressler, R. Rauch, and R. Reimann, Cryst. Res. Technol. 27 (1992) 413.
[3] C. W. King and O. H. Nestor, Proc. SPIE 1047 (1989) 80.
[4] I. T. Mouchovski, V. B. Genov, L. V. Pirgov, and V. Tz. Penev, Mat. Res. Innovat. 3 (1999) 138.
[5] L. B. Su, J. Xu, W. Q. Yang, Y. J. Dong, and G. Q. Zhou, J. Chin. Ceram. Soc. 31 (2003) 1202 (in Chinese).

[6] M. Verstraete and X. Gonze, Phys. Rev. B 68 (2003) 195123.
[7] Y. J. Dong, G. Q. Zhou, W. Q. Yang, L. B. Su, and J. Xu, J. Inorg. Mater. 19 (2004) 449 (in Chinese).
[8] H. Shi, R. I. Eglitis, and G. Borstel, Phys. Stat. Sol. B 242 (2005) 2041.
[9] V. Petit, J. L. Doualan, P. Camy, V. Menard, and R. Moncorge, Appl. Phys. B 78 (2004) 681.
[10] A. Lucca, G. Debourg, M. Jacquemet, *et al.*, Opt. Lett. 29 (2004) 2767.
[11] M. Pedroni, F. Piccinelli, T. Passuello, *et al.*, Nanoscale 3 (2011) 1456.
[12] L. B. Su, J. Xu, H. J. Li, *et al.*, Opt. Express 13 (2005) 5635.
[13] A. G. Nassiopoulou, V. Tsakiri, V. Ioannou-Sougleridis, *et al.*, J. Lumin. 80 (1999) 81.
[14] B. C. Hong and K. Kawano, Opt. Mater. 30 (2008) 952.
[15] F. Wang, X. P. Fan, D. B. Pi, and M. Q. Wang, Solid State Commun. 133 (2005) 775.
[16] Z. W. Quan, D. M. Yang, P. P. Yang, *et al.*, Inorg. Chem. 47 (2008) 9509.
[17] J. S. Wang, Z. W. Wang, X. Li, S. Wang, H. D. Mao, and Z. J. Li, Appl. Surf. Sci. 257 (2011) 7145.
[18] C. M. Zhang, C. X. Li, C. Peng, *et al.*, Chem. Eur. J. 16 (2010) 5672.
[19] C. Pandurangappa and B. N. Lakshminarasappa, Opt. Commun. 285 (2012) 2739.
[20] R. W. G. Wyckoff, Crystal Structures (Interscience/John Wiley, New York, 1963).
[21] M. D. Segall, P. J. D. Lindan, M. J. Probert, *et al.*, J. Phys.: Condens. Matt. 14 (2002) 2717.
[22] J. P. Perdew, K. Burke, and M. Ernzerhof, Phys. Rev. Lett. 77 (1996) 3865.
[23] D. Vanderbilt, Phys. Rev. B 41 (1990) 7892.
[24] H. J. Monkhorst and J. D. Pack, Phys. Rev. B 13 (1976) 5188.
[25] M. Verstraete and X. Gonze, Phys. Rev. B 68 (2003) 195123.
[26] G. W. Rubloff, Phys. Rev. B 5 (1972) 662.
[27] Y. J. Bi, Z. Y. Guo, H. Q. Sun, Z. Lin, and Y. C. Dong, Acta Phys. Sin. 57 (2008) 7800 (in Chinese).
[28] R. W. Godby, M. Schlüter, and L. J. Sham, Phys. Rev. B 37 (1988) 10159.
[29] M. S. Hybertsen and S. G. Louie, Phys. Rev. B 34 (1986) 5390.
[30] J. Bannon, Nature 157 (1946) 446.
[31] T. Tomiki and T. Miyata, J. Phys. Soc. Jpn. 27 (1969) 658.
[32] E. D. Palik, Handbook of Optical Constants of Solids (Academic Press, New York, 1991).
[33] G. W. Rubloff, Phys. Rev. B 5 (1972) 662.
[34] M. Fox, Optical Properties of Solids (Oxford University Press, New York, 2001).